Modelling, Simulation and Identification of Heat Loss Mechanisms for Parabolic Trough Receivers Installed in Concentrated Solar Power Plants

Simon Caron*, Marc Röger*

**German Aerospace Center (DLR), Institute for Solar Research, Plataforma Solar de Almería*
Tabernas 04200, Spain (Tel: +34 950 278 863; e-mail: simon.caron@ dlr.de)

Abstract: This paper describes a thermodynamic model library developed with the object-oriented language Modelica, which is both implemented for steady-state and transient heat transfer analyses of Parabolic Trough Receivers (PTRs) installed in Concentrated Solar Power (CSP) plants. For the identification of PTR heat loss mechanisms, this heat transfer model is coupled to a derivative-free hybrid optimization routine developed in Matlab, combining a Particle Swarm Optimization (PSO) algorithm with a Nelder-Mead Simplex (NMS) algorithm with search space boundary constraints.

Keywords: Thermodynamic Model, Model Validation, Transient Simulation, Parameter Identification.

1. INTRODUCTION

Parabolic Trough Receivers (PTRs) represent one of the key components in Concentrated Solar Power (CSP) plants, as their thermal performance significantly influences the solar field operating temperature and thus the power plant overall thermal efficiency. The development of an accurate in-situ receiver heat loss measurement method requires a numerical heat transfer model (Price et al., 2006), (Lüpfert et al., 2008) to separate heat loss mechanisms (Röger et al., 2014).

Several receiver heat transfer models have been published in the literature. Two-dimensional heat transfer models based on thermal resistance networks have been implemented with Engineering Equation Solver (EES) and validated under steady-state conditions (Forristall, 2003), (Kalogirou, 2012). More detailed three-dimensional models combining Finite Element Method (FEM), Computational Fluid Dynamics (CFD), and Monte Carlo Ray-Tracing (MCRT) have also been implemented with ANSYS (Wirz et al, 2012) and are more suitable for sun irradiated receivers (Eck et al., 2010).

This paper describes a three-dimensional receiver model library which has been extended from two-dimensional models (Forristall, 2003), (Kalogirou, 2012). This model has been implemented with Modelica, an object-oriented language designed for modelling complex physical systems. Steady-state and transient simulations have been performed for single receivers within Dymola simulation environment.

This receiver model has been validated for steady-state temperature conditions and has been coupled to a derivative-free hybrid optimization routine developed in Matlab in order to identify receiver heat loss mechanisms on the basis of transient measurements. The optimization routine combines a Particle Swarm Optimization (PSO) algorithm and a Nelder-Mead Simplex (NMS) optimization algorithm including search space boundary constraints.

2. THERMODYNAMIC MODEL

2.1 Heat loss balance

A typical PTR is made of two concentrical tubes. The inner stainless steel tube absorbs concentrated solar irradiation and transfers the heat to a fluid. The outer borosilicate glass envelope transmits solar irradiation and protects the absorber tube. A selective coating is typically applied on the outer absorber surface to reduce thermal radiation exchange while absorbing as much solar irradiation as possible. The annulus between both tubes is evacuated to reduce convective thermal losses. Both tubes are sealed with vacuum tight bellows on each ends, which compensate for the thermal expansion of the absorber at high operating temperatures.

A radial cross-section of a non-irradiated PTR is illustrated in Fig.1 (Lei et al., 2013) with radial heat flows.

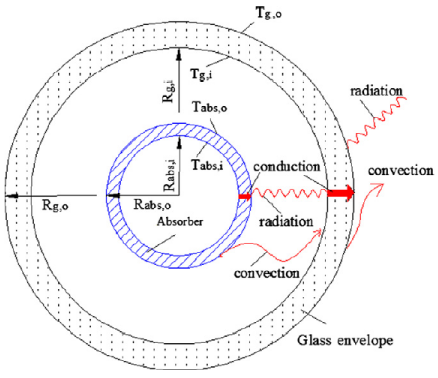

Fig. 1: Receiver cross-section and radial heat flows.

The model includes the radial heat flows illustrated in Fig.1 as well as circumferential and longitudinal conduction terms. The PTR geometry is discretized in cylindrical coordinates. Relevant heat flows are listed in Table 1. Heat flow model assumptions are described in (Röger et al., 2014).

Table 1. List of modeled heat flows

Heat flow	Heat Transfer from … to…		Mechanism
$\dot{q}_{cond,abs}$ (W)	Absorber (inner to outer surface) Temperatures: $T_{abs,i}$ (K); $T_{abs,o}$ (K)		Conduction (3D)
$\dot{q}_{rad,abs\text{-}gl}$ (W)	Absorber (outer surface) $T_{abs,o}$ (K)	Envelope (inner surface) $T_{gl,i}$ (K)	Radiation (1D)
$\dot{q}_{rad,abs\text{-}amb}$ (W)	Absorber (outer surface) $T_{abs,o}$ (K)	Ambient (Sky temp.) T_{sky} (K)	Radiation (1D)
$\dot{q}_{conv,abs\text{-}gl}$ (W)	Absorber (outer surface) $T_{abs,o}$ (K)	Envelope (inner surface) $T_{gl,i}$ (K)	Convection (1D)
$\dot{q}_{cond,gl}$ (W)	Envelope (inner to outer surface) Temperatures: $T_{gl,i}$ (K); $T_{gl,o}$ (K)		Conduction (3D)
$\dot{q}_{rad,gl\text{-}amb}$ (W)	Envelope (outer surface) $T_{gl,o}$ (K)	Ambient (Sky temp.) T_{sky} (K)	Radiation (1D)
$\dot{q}_{conv,gl\text{-}amb}$ (W)	Envelope (outer surface) $T_{gl,o}$ (K)	Ambient (air temp.) T_{air} (K)	Convection (1D)

The heat loss balance is expressed in the equation set (1-4) for a non-irradiated PTR with isolated bellows and a semi-transparent glass envelope.

$$\dot{q}_{cond,abs} = \dot{q}_{rad,abs\text{-}gl} + \dot{q}_{conv,abs\text{-}gl} \quad (1)$$

$$\dot{q}_{rad,abs\text{-}gl} + \dot{q}_{conv,abs\text{-}gl} = \dot{q}_{cond,gl} \quad (2)$$

$$\dot{q}_{cond,gl} = \dot{q}_{rad,gl\text{-}amb} + \dot{q}_{conv,gl\text{-}amb} \quad (3)$$

$$\dot{q}_{rad,abs\text{-}amb} + \dot{q}_{cond,gl} = \dot{q}_{loss} \quad (4)$$

where $\dot{q}_{loss}$ (W) corresponds to the PTR overall heat loss. This heat loss can be normalized by the PTR nominal length L (m) and is identified as the specific PTR heat loss $\dot{q}'_{loss}$ (W/m).

The transient heat loss balance for the glass envelope is expressed in Equation (5-7):

$$\rho_g c_{p,g} V_g \frac{dT_{gl}}{dt} = \dot{Q}_i + \dot{Q}_o \quad (5)$$

$$\dot{Q}_i = \dot{q}_{rad,abs\text{-}gl} + \dot{q}_{conv,abs\text{-}gl} = \dot{q}_{cond,gl} \quad (6)$$

$$\dot{Q}_o = \dot{q}_{rad,gl\text{-}amb} + \dot{q}_{conv,gl\text{-}amb} = \dot{q}_{cond,gl} \quad (7)$$

where ρ_g, $c_{p,g}$ and V_g respectively correspond to the glass density (kg/m^3), the glass specific heat capacity (J/kg.K) and the glass volume (m^3). Equations (6-8) are implemented in Modelica to derive the glass envelope temperature.

2.2 Internal heat loss mechanisms

Combining equations (1-5), the PTR overall heat loss can be expressed as the sum of three internal heat loss mechanisms: (i) thermal radiation exchange between the absorber and the envelope $\dot{q}_{rad,abs\text{-}gl}$ (W), (ii) annulus convection $\dot{q}_{conv,abs\text{-}gl}$ (W) and (iii) thermal radiation exchange between the absorber and the ambient $\dot{q}_{rad,abs\text{-}amb}$ (W).

The thermal radiation exchange $\dot{q}_{rad,abs\text{-}gl}$ is expressed for diffuse radiating surfaces (Siegel et al., 1981) in Eq. (8):

$$\dot{q}_{rad,abs\text{-}gl} = \frac{2\pi R_{abs,o} L \varepsilon_{abs} \varepsilon_{gl} \sigma}{\varepsilon_{gl} + \varepsilon_{abs}(1-\varepsilon_{gl}).\frac{R_{abs,o}}{R_{gl,i}}} (T^4_{abs,o} - T^4_{gl,i}) \quad (8)$$

where σ is Stefan-Boltzmann constant, ε denotes emittance values and R denotes geometrical radii for the corresponding surface. The absorber thermal emittance ε_{abs} (%) is a key PTR thermal property. This property is a function of the absorber temperature T_{abs} (K).

The annulus convection $\dot{q}_{conv,abs\text{-}gl}$ is expressed in Eq. (9):

$$\dot{q}_{conv,abs\text{-}gl} = 2\pi R_{abs,o} L h_{ann}.(T_{abs,o} - T_{gl,i}) \quad (9)$$

where h_{ann} (W/m^2.K) is a key PTR thermal property corresponding to the annulus heat transfer coefficient. This coefficient depends on the annulus pressure (Ratzel et al., 1979) and also on gas thermophysical properties (Burkholder, 2011). The nonlinear relationship between the annulus heat transfer coefficient and the annulus pressure is illustrated for four different gases in Fig. 2.

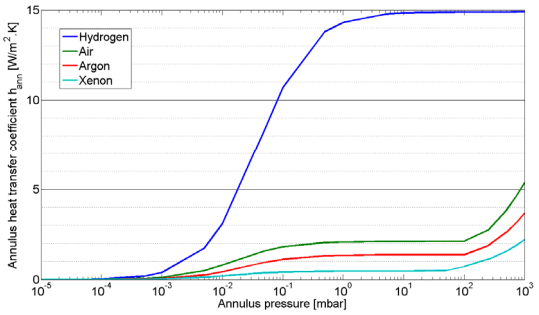

Fig.2: Simulation of annulus convective heat transfer. Fluid thermophysical properties derived from (Kleiber et al., 2010). Boundary conditions: T_{abs}=350°C, ε_{abs} = 10%, T_{amb} = 25°C, v_{wind} = 0 m/s. Receiver cross-sectional geometry: $R_{abs,i}$ = 33 mm; $R_{abs,o}$ = 35 mm; $R_{gl,i}$ = 59.5 mm; $R_{gl,o}$ = 62.5 mm.

3. MODELICA LIBRARY

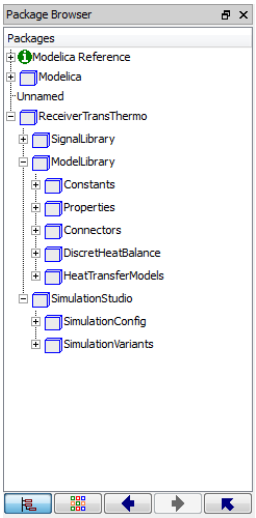

Fig. 3: ReceiverTransThermo Modelica Library.

3.1 Library components

The PTR Modelica library is named *ReceiverTransThermo* and its structure is displayed above in Fig.3. This library includes a first package *SignalLibrary* for transient analyses

based on the standard package *Modelica.Blocks.Sources*. The second package *ModelLibrary* includes custom material properties for the absorber tube, glass envelope, heat transfer fluid (HTF) and the annulus gas. It also includes the definition of thermal connectors, inherited from the package *Modelica.HeatTransfer.Interfaces*, as well as the definition of the 3D cylindrical discretization scheme. Finally, it includes the relevant heat transfer models for thermal simulations in steady-state and transient regimes.

3.2 Simulation Studio Package

The package *SimulationStudio* (Fig.3) includes two packages: *SimulationConfig* and *SimulationVariants*.

SimulationConfig includes basic configuration parameters and simulation kernels for two configurations: (i) a default PTR simulation configuration for stationary measurements and (ii) another configuration including a radiation shield designed for transient measurements, in which a portion of the PTR is isolated from the ambient environment. Each kernel configuration includes the basic interconnection of heat transfer models for the cylindrical discretization scheme.

SimulationVariants includes simulation variants, where relevant simulation boundary conditions are respectively defined for laboratory and field experiments. Each simulation variant can be opened within Dymola simulation environment for parametric studies and allows steady-state and transient thermal simulations.

4. STEADY-STATE SIMULATION

4.1 Experimental set-up

Laboratory test benches for PTR thermal characterization are described in (Burkholder et al., 2009), (Lei et al., 2013). The experimental set-up for steady-state heat loss measurements is illustrated in Fig. 4. The absorber inner surface is heated up with an electrical power to a certain temperature $T_{abs,i}$. Its bellows are isolated, so that adiabatic boundary conditions can be applied at the receiver end faces. At thermal equilibrium, the glass envelope outer temperature $T_{gl,o}$ remains constant and the electrical power P_{el} corresponds to the PTR heat loss $\dot{q}_{loss}$.

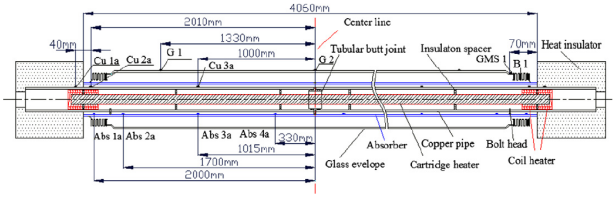

Fig. 4: Receiver Heat Loss Test Bench (Lei et al., 2013).

4.2 Model validation

The object-oriented receiver model can be used to simulate the PTR specific heat loss $\dot{q}'_{loss}$ as well as the glass envelope temperature $T_{gl,o}$ for stationary boundary conditions, i.e. an ambient temperature T_{amb} set to 25°C and a wind speed v_{wind} set to 0 m/s. The main model inputs are:

- the receiver geometry (Fig. 1)
- the absorber thermal emittance ε_{abs} (%)
- the annulus gas composition (Fig.2)
- the annulus pressure p_{ann} (mbar)
- the absorber temperature T_{abs}.

Isothermal temperature distributions are further assumed for the absorber tube and the glass envelope. For standard manufactured PTRs, the annulus is assumed to be sufficiently evacuated, so that gas thermal conduction can be neglected ($p_{ann} < 10^{-4}$ mbar).

Specific heat loss and glass envelope temperature simulated with the physical model are compared in Fig. (5-6) against experimental data obtained for two industrial receivers, i.e. Schott 2008 PTR70 tubes (Burkholder et al., 2009) and Himin PTR-2011 tubes (Lei et al., 2013). Calculated absorber thermal emittance values are used for these simulations. These emittance values were calculated from experimental data using Eq. (1). In addition, the glass envelope was assumed to be semi-transparent and a small fraction of the radiation emitted by the absorber was allowed to leak to the ambient through the glass envelope.

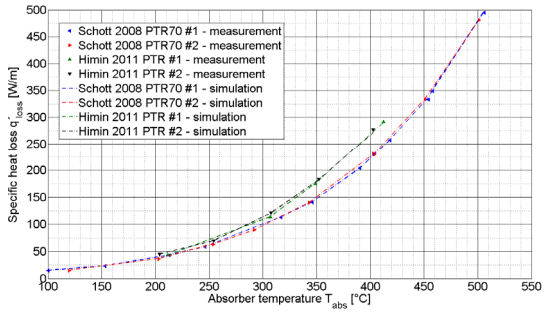

Fig. 5: Comparison between specific heat loss measurements and steady-state simulation results.

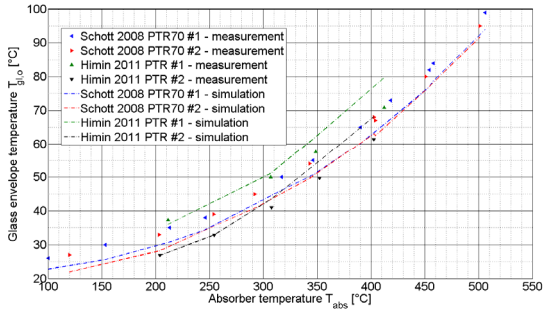

Fig. 6: Comparison between glass envelope temperature measurements and steady-state simulation results.

On the one hand, a good agreement can be observed between specific heat loss measurements and steady-state simulation results (Fig. 5).On the other hand, residual discrepancies can be observed between glass temperature measurements and steady-state simulation results (Fig. 6). The glass temperature remains a sensitive measurand, which depends not only on PTR key thermal properties, but on other ambient parameters (ambient temperature, sky temperature) and glass properties (thermal conductivity, opacity to infrared radiation).

5. TRANSIENT SIMULATION

5.1 Experimental set-up

An alternative PTR heat loss measurement technique based on transient infrared thermography was described in (Röger et al., 2014) and further investigated in (Caron et al., 2014). The experimental set-up is illustrated in Fig. 7. A radiation shield is mounted around the PTR, reflecting the radiation heat flow $\dot{q}_{rad,gl\text{-}amb}$ towards the glass envelope. Two infrared pyrometers respectively measure the absorber outer surface temperature through the glass envelope in the wavelength range from 2.0 to 2.6 µm and the glass envelope outer surface temperature in the wavelength range from 8 to 14 µm.

A transient excitation is applied to the absorber temperature and the glass temperature response is recorded under stable ambient conditions. The relationship between the absorber temperature excitation and the glass temperature response is analysed to determine the PTR key thermal properties.

One advantage of the transient heat loss measurement principle over steady-state heat loss measurements is that it can be implemented for in-situ PTR thermal characterization in CSP plants. Another advantage offered by the transient measurement technique in comparison to steady-state heat loss measurements is the separation of internal heat loss mechanisms, using the PTR thermodynamic model library.

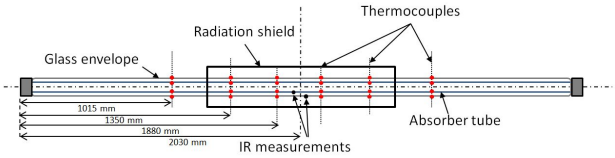

Fig. 7: Transient infrared thermography experimental set-up.

5.2 Modelling approach

The thermal behaviour of a PTR can be modelled as a Linear Time Invariant (LTI) system. A single-input, single-output (SISO) complex transfer function *F(jω)* can be defined, which relates the glass envelope temperature $T_{gl}(t)$ to the absorber temperature $T_{abs}(t)$. For stable ambient conditions, a first order system transfer function (Eq. 10) can be assumed. This approach allows the derivation of two measurands at a given angular frequency ω (rad/s), namely the amplitude ratio *A* (-) and the phase shift *φ* (rad) (Eq. 11).

$$F(j\omega) = \frac{G}{1 + j\omega\tau} \tag{10}$$

$$|A(\omega)| = \frac{G}{\sqrt{1 + \omega^2\tau^2}}; \varphi(\omega) = -tan^{-1}(\omega\tau) \tag{11}$$

These two measurands are derived at a given working point (WP), defined by the following three measurands:

- mean absorber temperature $\overline{T_{abs,o}}$ (K)
- mean glass envelope temperature $\overline{T_{gl,o}}$ (K)
- mean air temperature inside the ventilated radiation shield enclosure $\overline{T_{air,shield}}$ (K)

The PTR key thermal properties ε_{abs} (%) and h_{ann} (W/m^2.K) can be first expressed as implicit bijective functions, respectively f_1 (Eq. 12) and f_2 (Eq. 13), of the five measurands {A, φ, $\overline{T_{abs,o}}$, $\overline{T_{gl,o}}$, $\overline{T_{air,shield}}$} described above.

$$\varepsilon_{abs} = f_1(A, \varphi, \overline{T_{abs,o}}, \overline{T_{gl,o}}, \overline{T_{air,shield}}) \tag{12}$$

$$h_{ann} = f_2(A, \varphi, \overline{T_{abs,o}}, \overline{T_{gl,o}}, \overline{T_{air,shield}}) \tag{13}$$

5.3 Transient temperature profiles

Two types of transient absorber temperature excitations were investigated in (Caron et al., 2014), namely sinusoidal and ramp-and-hold profiles. The glass temperature response can be simulated with Dymola for given boundary conditions, as illustrated in Fig.8 (Sinus) and Fig. 9 (Ramp-and-hold). The thermodynamic model includes convection and radiation heat transfer models for the radiation shield enclosure.

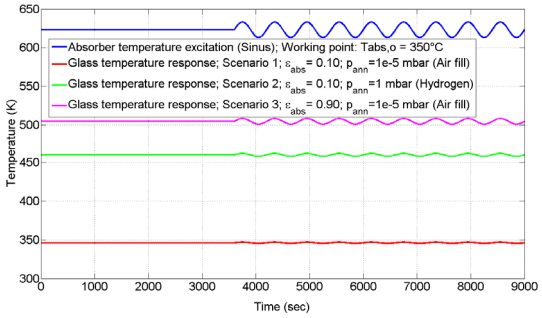

Fig. 8: Transient temperature profiles, Sinus excitation.

According to LTI system theory, the glass envelope shows a sinusoidal temperature response for a sinusoidal excitation (Fig. 8). One can qualitatively observe that the amplitude ratio $|A(\omega)|$ increases as PTR heat losses increase from *Scenario 1* to *Scenario 3*, while the phase shift magnitude $|\varphi(\omega)|$ decreases.

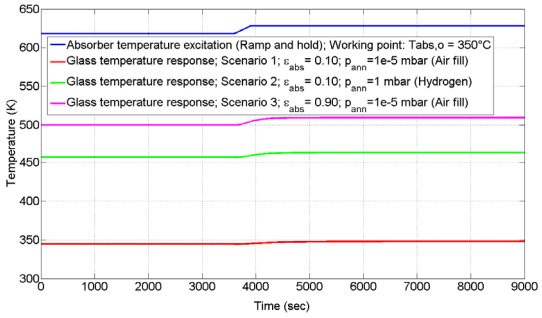

Fig. 9: Transient temperature profiles, Ramp-and-hold.

According to LTI system theory, the glass temperature response follows a nearly sigmoidal profile for ramp-and-hold excitations (Fig.9). The glass temperature response can be analysed for a broad range of angular frequencies, as illustrated in Fig. 10 and Fig. 11.

The angular frequency ω is first set equal to the value previously defined for sinusoidal measurements, here 600 seconds, in order to allow a direct comparison between both types of excitation.

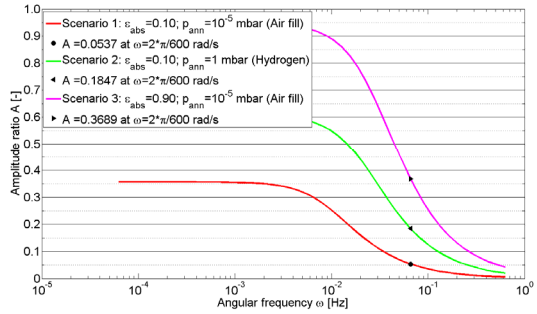

Fig. 10: Illustration of the amplitude ratio Bode diagram for distinct PTR transfer functions.

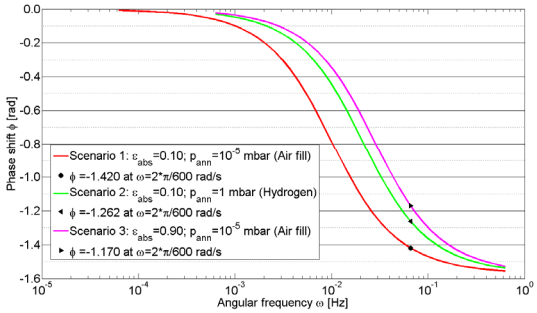

Fig. 11: Illustration of the phase shift Bode diagram for distinct PTR transfer functions.

6. PARAMETER IDENTIFICATION

6.1 Identification problem

The transient heat loss analysis workflow is summarized in Fig. 12. The PTR key thermal properties ε_{abs} *(%) and* h_{ann} *(W/m².K)* are implicit functions of transient measurands (see Eq. 12-13). The derivation of PTR key thermal properties is achieved by parameter identification, which is further explained in this section. PTR key thermal properties are necessary to simulate the specific heat loss $\dot{q}'_{loss}$ of a PTR at standard ambient conditions, i.e. the ambient temperature T_{amb} is set to 25°C and the wind speed v_{wind} is set to 0 m/s.

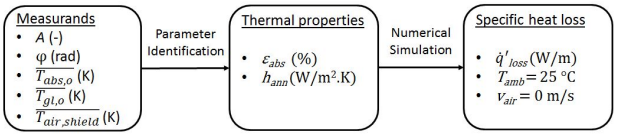

Fig. 12: Transient heat loss analysis workflow.

The implicit functions f_1 (Eq. 12) and f_2 (Eq. 13) are a priori unknown. One option for the identification of key thermal properties would be to generate look-up tables with the PTR heat transfer model for various transient measurands value sets. This first solution is associated with high computation costs, if one wishes a fine resolution.

Another option presented in (Röger et al., 2014) consists in deriving an analytical model by linearizing the differential equation (Eq. 6) and neglecting the radiative heat flow between the glass envelope and the radiation shield. While this approach works reasonably well for standard receivers, it fails at capturing the strong non-linearities for degraded PTRs with high emittance coatings or non-evacuated annuli.

The last investigated option is to couple the PTR numerical model with an optimization routine. The optimization routine is based on a hybridation of derivative-free algorithms and it searches for a parameter combination that best reproduces experimental measurands by simulation.

6.2 Optimization routine

Relevant model parameters for the optimization routine are:

- the absorber thermal emittance ε_{abs} (%)
- the annulus heat transfer coefficient hann (W/m².K)
- the mean absorber temperature $\overline{T_{abs,o}}$ (K)
- the mean air temperature $\overline{T_{air,shield}}$ (K)
- the mean air velocity v_{air} (m/s) inside the shield

The objective function δ^2 is defined as the sum of squared relative deviations Δ_i (%), where the individual deviations Δ_i correspond to the respective deviations between simulated and experimental measurands ($X_{i,sim} - X_{i,meas}$), normalized by the measurand ($X_{i,meas}$) (Caron et al., 2014). The equations for the objective function are formulated in Eq. (14-15):

$$\delta^2 = \sum_{i=1}^{5} \Delta_i^2 \; ; \; \Delta_i = \frac{X_{i,sim} - X_{i,meas}}{X_{i,meas}} \tag{14}$$

$$X = \{A(-), \varphi(rad), \overline{T_{abs,o}}(K), \overline{T_{gl,o}}(K), \overline{T_{air,shield}}(K)\} \tag{15}$$

The optimization routine is programmed in Matlab and it is coupled with Dymola. This routine sequentially combines a Particle Swarm Optimization (PSO) algorithm with a Nelder Mead Simplex (NMS) optimization algorithm with search space boundary constraints. As PTR key thermal properties are a priori unknown, the parameter search first starts within a broad search space, which is partitioned in complementary subspaces with regard to the annulus pressure (Fig. 2). After a first global PSO (10 particles, 10 rounds per subspace), the subspaces are further restricted with respect to the parameter ε_{abs}. A second PSO (10 particles, 10 rounds per subspace) further improves the candidate starting points for the NMS (Max. 200 iterations).

Each subspace is handled in an individual Matlab session to allow a faster convergence via parallel computation. With four parallel subspaces and an Intel Core i7 processor with 4 threads, the optimization converges in less than 2 hours.

6.3 Identification results

The identification of PTR key thermal properties was carried out for laboratory sinusoidal measurements and documented in (Caron et al., 2014) for three different receiver categories. Specific heat loss experimental results are shown in Fig. 13 and compared both with steady-state measurements and simulations based on material data.

A good agreement can be observed between transient derived specific heat losses and steady-state measurements for PTRs with high emittance coatings (Category B, Category C). Relative deviations respectively ranged from -9.0% to -3.0%

for evacuated PTRs (Cat. B) and from -1.7% to 1.3% for non-evacuated PTRs (Cat. C). For these PTRs, low values could be achieved for the objective function δ^2 (below 1e-5).

The quality of the agreement degraded for standard PTRs with selective absorber coating and evacuated annuli (Category A). The relative deviations between transient and steady-state specific heat losses ranged from 8.8% to 27.4% and increased significantly with higher operating absorber temperatures. For these PTRs, higher values were reached for the objective function δ^2 (below 2e-2), thus indicating a potential for improvements in the transient model calibration.

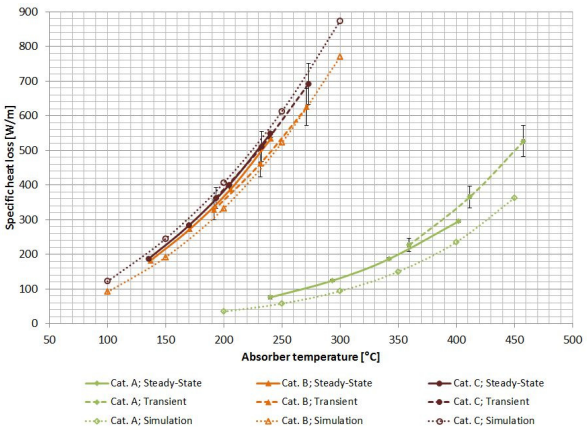

Fig. 13: Comparison between steady-state specific heat loss measurements (*Steady-State*), transient derived specific heat losses (*Transient*) and simulates specific heat losses based on material data (*Simulation*).

8. CONCLUSION

This paper presented a parabolic trough receiver heat transfer model implemented with the object-oriented language Modelica. This physical model could be used for receiver design and parameter studies.

This numerical model was validated for steady-state experimental data and extended for transient simulations. A parameter identification algorithm based on derivative-free optimization algorithms was developed with Matlab and coupled to Dymola to determine key receiver thermal properties from transient measurands.

The object-oriented model offers great flexibility and heat transfer models can be further refined to capture detailed dynamic heat transfer characteristics. The optimization criterium and objective function could be simplified further to allow a direct identification of receiver thermal properties for noisy datasets gained during field measurements. This new procedure is being implemented for noisy datasets where the derivation of transient measurements is less trivial.

ACKNOWLEDGMENTS

Financial support from the German Federal Ministry for Economic Affairs and Energy (PARESO, Contract 0325412) is gratefully acknowledged. The author also thanks Dr. Ricardo Silva from CIEMAT-UAL research group for his valuable insights on optimization algorithms.

REFERENCES

Burkholder, F., Kutscher, C. (2009), Heat Loss Testing of Schott's 2008 PTR70 Parabolic Trough Receiver, *NREL Technical Report NREL/TP-550-4533*.

Burkholder, F. (2011), Transition Regime Heat Conduction of Argon/Hydrogen and Xenon/Hydrogen Mixtures in a Parabolic Trough Receiver*, Ph.D Thesis, University of Colorado, United States*.

Caron, S., Röger, M., Pernpeintner, J. (2014), Transient Infrared Thermography Heat Loss Measurements on Parabolic Trough Receivers Under Laboratory Conditions, Paper presented at the *SolarPACES 2014 Conference*, 16-19 September 2014, Beijing, China.

Eck, M., Feldhoff, J.F., Uhlig, R. (2010), Thermal Modelling and Simulation of Parabolic Trough Receiver Tubes, *ASME 2010 International Conference of Energy Sustainability Proceedings*, pp. 659-666.

Forristall, R. (2003), Heat Transfer Analysis and Modelling of a Parabolic Trough Solar Receiver Implemented in Engineering Equation Solver, *NREL Technical Paper NREL/TP-550-34169*.

Kalogirou, S.A. (2012), A detailed thermal model of a parabolic trough collector receiver, *Energy*, Vol. (48), pp. 298-306.

Kleiber, M., Joh, R. (2010), *VDI Heat Atlas*, *Chapter D 3.1, Properties of Pure Fluid Substances; Liquids and Gases*. Springer-Verlag, Berlin Heidelberg.

Lei, D., Li, Q., Wang, Z., Li,J., Li,J. (2013), An experimental study of thermal characterization of parabolic trough receivers, *Energy Conversion and Management*, Vol. (69), pp. 107-115.

Lüpfert, E., Riffelmann, K.J., Price, H., Burkholder, F., Moss, T. (2008), Experimental Analysis of Overall Thermal Properties of Parabolic Trough Receivers, *ASME Journal of Solar Energy Engineering*, Vol. (130), pp. 021007-1: 021007-5.

Price, H., Forristall, R., Wendelin, T., Lewandowski, A., Moss, T., Gummo, C. (2006), Field Survey of Parabolic Trough Receiver Thermal Performance, *ASME 2006 International Solar Energy Conference Proceedings*, pp. 109-116.

Ratzel,A.C.,Hickox, C.E.,Gartling, D.K. (1979), Techniques for Reducing Thermal Conduction and Natural Convection Heat Losees in Annular Receiver Geometries, *ASME Journal of Heat Transfer*, Vol. (101), pp.108-113.

Röger, M., Potzel, P., Pernpeintner, J., Caron, S. (2014), A Transient Thermography Method to Separate Heat Loss Mechanisms in Parabolic Trough Receivers, *ASME Journal of Solar Energy Engineering*, Vol. (136), pp.011006-1:011006-9.

Siegel, R., and Howell, J. R., (1981), *Thermal Radiation Heat Transfer*, 2nd edition, McGraw-Hill, New York.

Wirz,M.,Roesle, M.,Steinfeld, A. (2012), Three-Dimensional Optical and Thermal Numerical Model of Solar Tubular Receivers in Parabolic Trough Concentrators, *ASME Journal of Solar Energy Engineering*, Vol. (134), pp. 041012-1:041012-9.